

On the Real-World Performance of

Harald Songoro - SEMCAD X Group - Schmid & Partner Engineering AG - Switzerland

INTRODUCTION

Lately, the Finite Difference Time Domain (FDTD) method [6] has gained increased interest due to its ability to simulate complex models for a wide range of applications. However, its time integration scheme is bound to a stability criteria that can become exceedingly small for models with very fine geometrical features. This shortcoming is theoretically overcome by the Alternating Direction Implicit Finite Difference Time Domain method for Maxwell's equations (ADI-FDTD) [2,3,4]. ADI-FDTD is an approximate factorization of the Crank-Nicholson scheme (CN) applied to Yee discretization. It retains the unconditional stability and the second order of accuracy of CN while leading to a lower computational cost that makes it attractive.

However, the additional error introduced by that factorization can become a dominant term of the truncation error for large time-steps and/or at material interfaces, making the accuracy of ADI-FDTD difficult to predict.

Therefore, the objective of this study was to assess the performance of ADI-FDTD for real-world applications.

METHODS

An ADI-FDTD\FDTD solver has been integrated into [6], a 3D CAD EM simulation platform, enabling us to simulate complex applications for which ADI-FDTD is likely to be more efficient than FDTD. One of the key issues when using ADI-FDTD is the choice of the time step, which is no longer driven by a stability criteria nor by the Nyquist limit but by the research of a compromise between an acceptable truncation error and a competitive simulation time compared to FDTD. Such a time step has been chosen by default for all ADI-FDTD simulations and is given by:

$$\Delta t = CFL_{\min} \times \sqrt{\frac{CFL_{\max}}{CFL_{\min}}}$$

THE ADI-FDTD\FDTD SOLVER

The ADI-FDTD and FDTD methods have been merged and implemented within the same solver. Both methods share the same spatial discretization and modeling features, thus excluding from the comparison the influence of factors external to the time integration schemes.

The computational domain is truncated by the UPML [5] absorbing boundary condition modified in order to retain the unconditional stability of ADI-FDTD. Typical modeling features [6] such as plane wave excitations, voltage sources and R,L,C lumped elements have also been included.

solver optimizations	computation speed million voxels per s	allocated memory bytes per voxel
one-time factorization stored in memory	1 - 1.2	300 - 320
re-factorized at each iteration	0.75 - 0.85	100 - 130

Performance overview of the ADI-FDTD solver on a P4 3.4Ghz

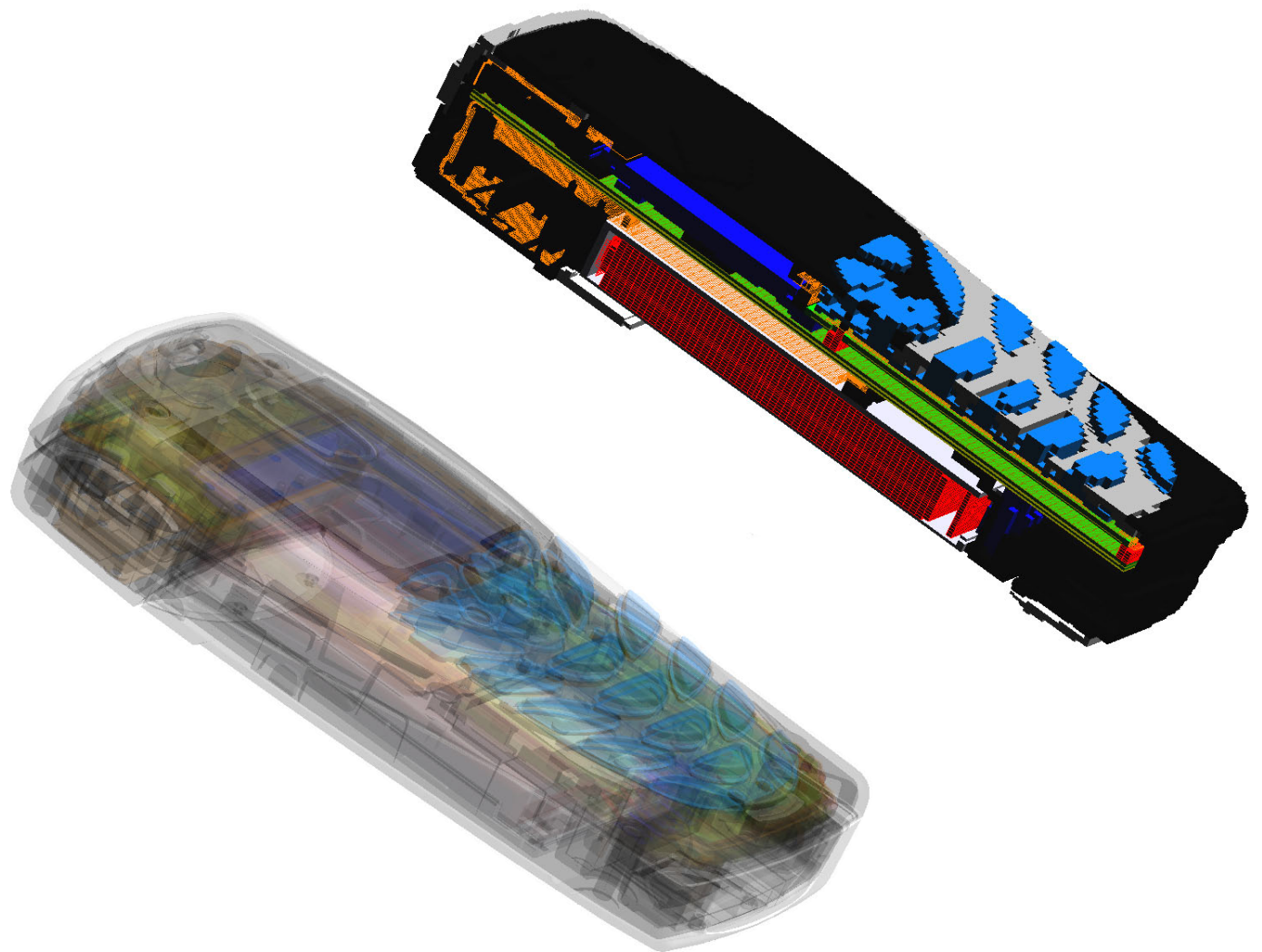
BENCHMARKS

In the following benchmarks, ADI-FDTD simulations have been run for different time steps and are compared with their corresponding FDTD simulation (used as the reference simulation). The time steps of the ADI-FDTD simulations are specified as multiples of the CFL criteria.

All excitations are harmonic, and all fields are extracted in the frequency domain.

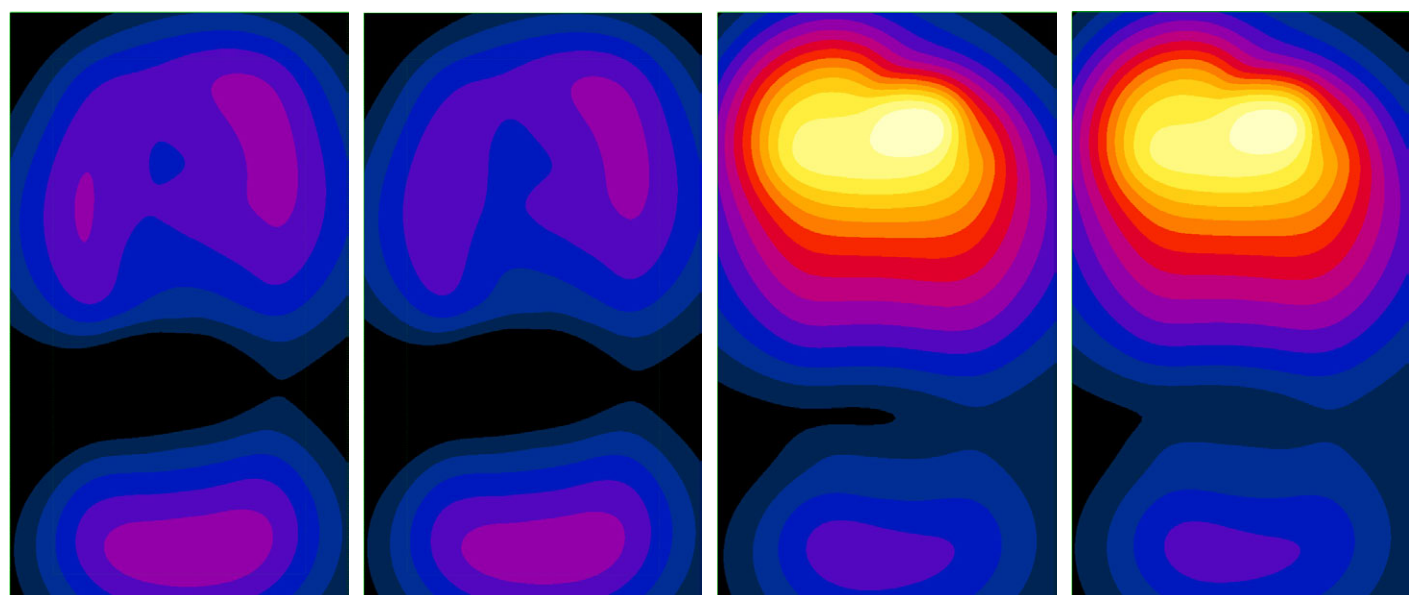
Comparisons between ADI-FDTD simulations and the FDTD reference simulation bear on E field modules or H field modules and are characterized by their deviation calculated by

$$D = \frac{\|E_{rms}^{ADI-FDTD} - E_{rms}^{FDTD}\|_2}{\|E_{rms}^{FDTD}\|_2}$$



CAD model and discretized model of the NOKIA 8310

The mesh is truncated by 8 layers of UPML media leading to an overall mesh size of 5.6 million voxels whose size varies between 0.01 mm and 12 mm. The default time step is 32CFL.



FDTD simulation
E-field distribution in front plane

ADI-FDTD 32CFL simulation
E-field distribution in front plane

FDTD simulation
E-field distribution in back plane

ADI-FDTD 32CFL simulation
E-field distribution in back plane

BENCHMARK 1: NOKIA 8310

Our objective was to replicate with the ADI-FDTD solver a previous joint study carried out with the Nokia Research Center (NRC, Finland) aiming at evaluating to which degree FDTD is capable of accurately simulating an entire CAD derived model (CATIA) of the NOKIA 8310.

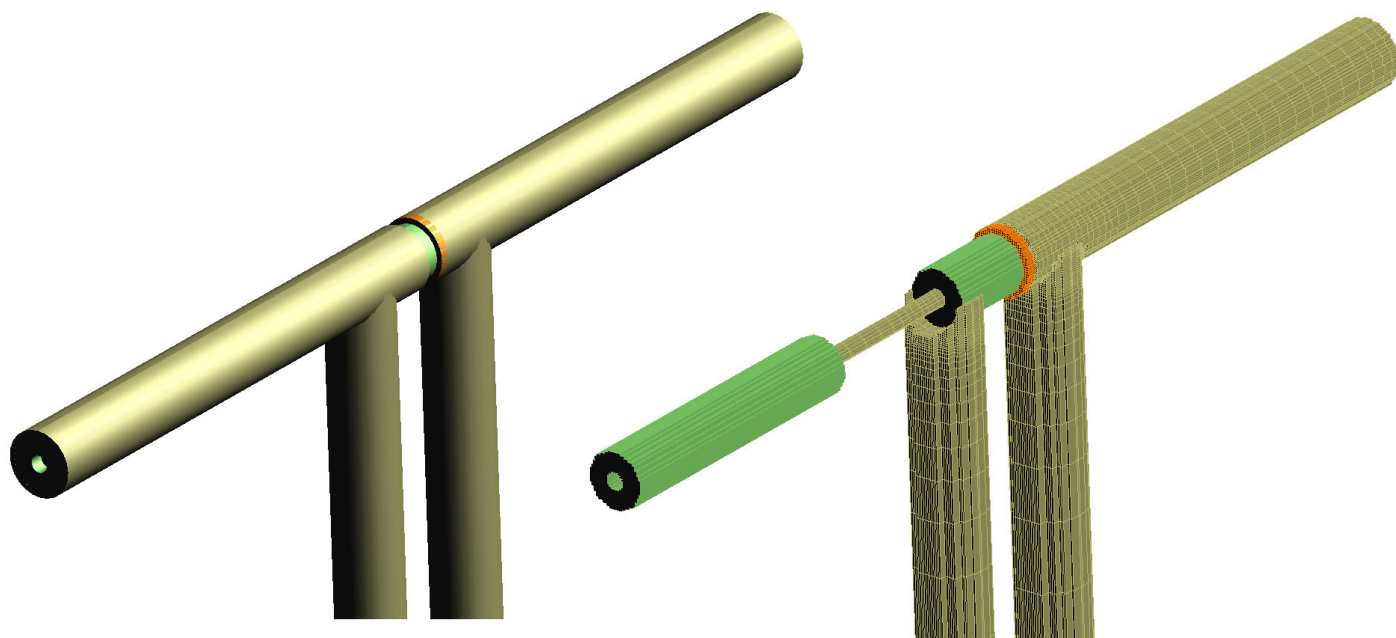
An important aspect of this study concerns the near-field analysis in which E-fields (dB normalized to maximum) are compared for the DCS1800 band in two horizontal planes located at 3 mm from either side of the phone.

Both ADI-FDTD and FDTD simulations show that the energy is mostly radiated out of the back of the phone through the high E-fields located above the antenna. This is desirable because the energy is thus directed away from the user, as intended with the use of an integrated antenna.

solver time step	FDTD CFL	ADI 4CFL	ADI 8CFL	ADI 16CFL	ADI 32CFL	ADI 48CFL
deviation of E front	0%	0.4%	0.5%	2.1%	2.6%	5.7%
deviation of E back	0%	0.07%	0.3%	0.6%	2.7%	6.1%
Antenna Efficiency	63%	63%	63%	62%	63%	62%

Benchmark results

The deviations between the FDTD reference simulation and the ADI-FDTD simulations are very small up to a time step of 32CFL. This benchmark shows not only that ADI-FDTD is as robust as FDTD for complex simulations but also that it is significantly more efficient.



CAD model and discretized model of the CD2450 dipole

The mesh is truncated by 6 to 8 layers of UPML media leading to an overall mesh size of 1.3 million voxels whose size varies between 0.09 mm and 8 mm. The default time step is 8CFL.

BENCHMARK 2: HAC CALIBRATION DIPOLE

The dipole under investigation is part of a set of calibration dipoles used within ANSI-PC63.19 (Hearing Aid Compatibility). In order to achieve the operational bandwidth as specified in the standard, the dipole construction includes internal dielectrics in the arms to broaden the frequency range of operation. An accurate representation of its structure therefore requires finely detailed discretization.

One essential part of the calibration procedure is the comparison of E-fields (dB normalized to maximum) in a plane at 10mm above the dipole.

Both ADI-FDTD and FDTD simulations show a field distribution that is typical of a dipole. This is desirable because the influence of the optimizations realized to

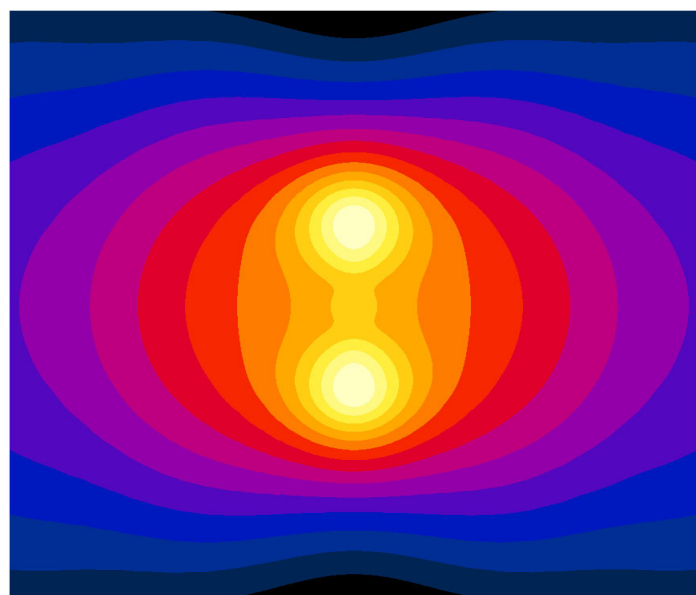
broaden the frequency range of operation must be minimized.

time step	1CFL	2CFL	4CFL	8CFL	16CFL	32CFL
deviation of E top	0.032%	0.28%	0.75%	1.4%	4.1%	9.1%

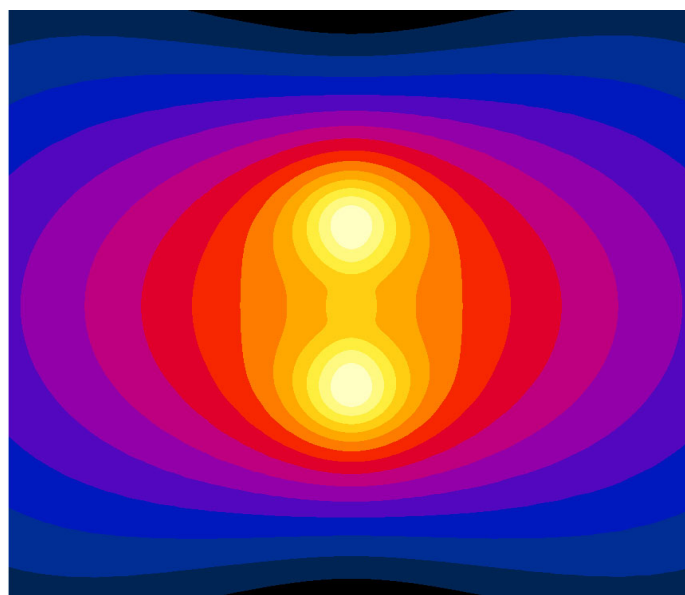
Benchmark results

The deviations between the FDTD reference simulation and the ADI-FDTD simulations are small up to a time step of 16CFL.

This benchmark shows that ADI-FDTD can also be advantageous for ordinary applications.



FDTD simulation
E-field distribution at 10 mm



ADI-FDTD 8CFL simulation
E-field distribution at 10 mm

CONCLUSIONS

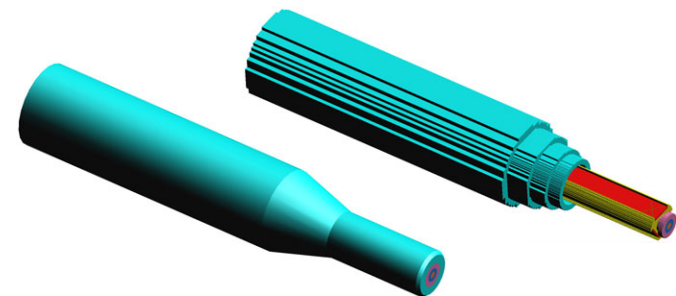
This study supports the use of ADI-FDTD for real-world applications.

The applicability and robustness of ADI-FDTD have been shown for large and complex 3D CAD based models.

ADI-FDTD was found to be more efficient than FDTD for locally over-discretized models.

BENCHMARK 3: ET3D DOSIMETRIC PROBE

ET3D is an isotropic E-field probe for dosimetric measurements from 10Mhz to 2Ghz. Our objective was to calculate its conversion factor at 13.56Mhz in a brain equivalent liquid with a relative permittivity of 80 and a conductivity of 0.75 S/m. To this end, ET3D was exposed to several incident plane waves propagating in air and in lossy liquid for three polarizations corresponding to the orientations of the three internal sensors.



CAD model and discretized model of the ET3D probe

The 1.8 mm internal sensors inside the probes (in green) are used to record the voltage. The mesh is truncated by 10 layers of UPML media, leading to an overall mesh size of 3.3 million voxels whose size varies between 0.04 mm and 12 mm. The default time step calculated is slightly above 50CFL.

The conversion factor depends on the frequency and on the electrical properties of the liquid. It relates the voltage measured by the sensors of the probe to the E-field at the probe location and is calculated by

$$CF(f) = \frac{UL_0^2(f) + UL_{120}^2(f) + UL_{240}^2(f)}{UA_0^2(f) + UA_{120}^2(f) + UA_{240}^2(f)} \cdot \frac{1}{E_{ref}^2(f)}$$

If θ is the polarization angle of the plane wave excitation $UL_\theta(f)$ is the voltage at the sensor location when the probe is placed inside the dosimetry liquid and $UA_\theta(f)$ is the voltage at the sensor location when the probe is in air; $E_{ref}^2(f)$ is the module of the electric field at the sensor location when there is no probe and is used to normalize the voltage in air and liquid for the same E-field amplitude of 1 V/m.

solver time step	FDTD CFL	ADI 25CFL	ADI 50CFL	ADI 75CFL	ADI 100CFL
$CF(13.56)$	9.0	9.3	9.7	10.1	10.5
deviation of E in air	0%	2.1%	4.9%	7.2%	9.3%
deviation of H in lossy liquid	0%	1.17%	1.7%	2.3%	3.2%

Benchmark results

The deviations between the FDTD reference simulation and the ADI-FDTD simulations are small up to a time step of 50CFL.

This benchmark shows that ADI-FDTD is also well suited for quasi-static applications such as plane wave excitations propagating in air or lossy background.

ACKNOWLEDGEMENTS

This study was generously supported by the Swiss Commission for Technology and Innovation (CTI). Moreover the author would like to acknowledge the support of S. Benkler², N. Chavannes², E. Cherubini¹, P. Futter¹, H. Gerber¹, J. Gubler², N. Kuster², K. Pokovic¹

¹Schmid & Partner Engineering AG - Zurich
²IT'IS Foundation - ETH Zurich

REFERENCES

- [1] A. Taflov and Susan C. Hagness, "Computational electrodynamics: the FDTD method, second edition", 2000.
- [2] Jim Douglas Jr., James E. Gunn, "A General Formulation of Alternating Direction Methods: Part I. Parabolic and Hyperbolic Problems", Numer. Math. Bd. 6, 1964.
- [3] T. Namiki, "A new FDTD algorithm based on alternating direction implicit method", IEEE Trans. Microwave Theory Tech., vol. 47, 999.
- [4] F. Zheng, Z. Chen, and J. Zhang, "A finite difference time domain method without the Courant stability conditions", Microwave Guided Wave Lett., vol. 9, 1999.
- [5] SEMCAD X, www.speag.com, Schmid & Partner Engineering AG.
- [6] S. Gedney, "An anisotropic perfectly matched layer absorbing media for the truncation of FDTD Lattices", IEEE Trans. Ant. Prop. vol., 44, 1996.